Pure Appl. Geophys. 174 (2017), 3979–4001

DOI 10.1007/s00024-017-1599-6

Pure and Applied Geophysics

Numerical Simulation of Wave Characteristics off Kulasekharapatnam, Southeast Coast of India

Umesh P. A,[1] Selvin P. Kani,[2] and Prasad K. Bhaskaran[1]

Abstract—Waves are important driving forces that have significant implications in deep and shallow waters. To achieve further understanding of the characteristics of wind waves in the Gulf of Mannar, an attempt is made based on the measured data off Kulasekharapatnam for the period from January 2006 to May 2007. The integrated third-generation ocean wave models, WAM and SWAN, are implemented to simulate the significant wave parameters. Simulations were carried out using ECMWF ERA-Interim winds over the deep waters (30°E–120°E; 70°S–30°N and 76°E–80°E; 6°N–10°N) domains. Comparison of the ECMWF ERA-Interim wind data against the field measured data demonstrates that the overall trend and dominant directions are consistent with the observational data. The validation of significant wave parameters exhibited very high correlation ($R > 0.9$) at the study location. Wave heights are high in the Gulf of Mannar during the southwest monsoon period and the waves are from south-southwest. The study also shows that swells are predominant (24%) in the Gulf of Mannar during non-monsoon period and during rest of the year, wind sea (75.9%) dominates. The study also demonstrates the sensitivity of the SWAN model towards different GEN3 physics options and bottom friction formulations by forcing the model with QuikSCAT/NCEP Blended winds off Kulasekharapatnam. The simulations obtained using different GEN3 physics options and bottom friction formulations have been compared with the buoy data. The study indicates that the SWAN model with Janssen and Komen physics options simulates the significant wave height and mean wave period, respectively, with a fairly high degree of accuracy. Similarly, the JONSWAP formulation for bottom friction reproduced the buoy signals at the study location with good accuracy for both significant wave height and mean wave period. The study demonstrates that the simulations are sensitive to the choice of GEN3 physics and bottom friction formulations off Kulasekharapatnam, and hence effective for obtaining more accurate wave predictions.

Key words: WAM, SWAN, Gulf of Mannar, wave model validation, Kulasekharapatnam.

1. Introduction

Ocean waves play an important role in the marine weather having profound implications on the coastal communities, shipping routes, and offshore industry. Wave climate refers to the general condition of the sea state of a specific location or over a coastal or offshore region. They also play an important role in sediment transport and shoreline evolution. Wave-induced currents are primarily responsible for transportation and deposition of near shore sediments (Castelle et al. 2006) considered in the design of coastal structures (Sorensen 1997). Waves are known to play an important role in the distribution of suspended sediment concentrations and bed form characteristics where accumulation of some classes of nutrients and pesticides are evident (Schneggenburger et al. 2000). Evaluation of wave characteristics during severe sea state is essential for adequate design and construction of coastal structures (Kumar et al. 2004). Therefore, the understanding of wind-waves is necessary for the planning, design and construction of new ports and harbors, coastal protection structures, navigational channels (Sundar and Ananth 1988), and also contributes in navigation, coastal development and planning. The knowledge of wind-waves is necessary to understand the behavior and occurrence of pelagic fish as well (Reddy 2001). The principal elements that are associated with wave climate are the significant wave parameters such as significant wave height (H_s), mean wave period (T_s) and mean wave direction.

Wave conditions in the Indian Seas (Arabian Sea and Bay of Bengal) solely depend on the strength of the monsoon (Swain 1997) and it is applicable to the Gulf of Mannar as well, as the area is influenced by the Indian monsoon system. Wave climate off the

[1] Department of Ocean Engineering and Naval Architecture, Indian Institute of Technology Kharagpur, Kharagpur, West Bengal 721 302, India. E-mail: prasadlsu@yahoo.com; pkbhaskaran@naval.iitkgp.ernet.in

[2] Integrated Coastal Zone Management Project, Institute of Environmental Studies and Wetland Management, Sector-1, Salt Lake City, Kolkata 700 064, India.

east coast of India is dominated by three different seasons, namely the southwest (SW) monsoon from June to September, the northeast (NE) monsoon from October to January and the fair-weather season from February to May. Among the three seasons during SW monsoon, the wave climate is generally rough (Chandramohan et al. 1993; Neetu et al. 2006). Wave characteristics along the east coast of India are studied by various researchers (Nayak et al. 1992; Kumar et al. 2003; Aboobacker et al. 2009). Along the Indian coast, about 60% of the wave spectra observed is multi-peaked (Kumar et al. 2003) due to the presence of seas and swells, and they are mainly single-peaked when the significant wave height is more than 2 m. The multi-peaked spectra are mainly due to the existence of wind seas along with the swells; and different methods are used for separation of wind sea and swell (Wang and Hwang 2011; Portilla et al. 2009). Along the east coast of India, the wave activity is significant both during SW and NE monsoons (Kumar et al. 2006). Cyclones frequently occur in the Bay of Bengal; and the 1964 Rameswaram cyclone is one of the severe storms (Rao and Mazumdar 1996) which affected Sri Lanka and the southern Indian peninsula. In the southeast coast of India, waves during the southwest (SW) monsoon have less significance compared to those during the northeast (NE) monsoon. Hence, it has become an important task to achieve a comprehensive understanding of the behavior and characteristics of waves in the region off Kulasekharapatnam to guide the planning, designing and implementing of projects in this area.

The state-of-art third-generation spectral wave models are WAM (WAMDIG 1988), WAVEWATCH III (Tolman 1991) and SWAN (Booij et al. 1999) which are used for operational wave forecasting over the globe. WAVEWATCH III and WAM model are deep water models and is widely used in studying the wave processes in oceans (Prasad Kumar et al. 2003; Prasad Kumar and Stone 2007; Nayak et al. 2013). However, the untransformed data at grid points in deep water provide poor estimates of wave characteristics in nearshore region. The SWAN model (Saket et al. 2013; Mazaheri et al. 2013) is designed to simulate the propagation of random, short-crested, wind-generated waves in coastal regions and inland shallow waters. It can deal with the complex wave transformations from bathymetry, wind, and other factors.

The study of wave characteristics off Kulasekharapatnam, as shown in Fig. 1, is important from many perspectives. The Southern Coromandel Coast (southeast Bay of Bengal coast—stretching from Pulicat to Kanyakumari) has a long history of shipping. Since historical times, this portion of the coast (Palk Bay and Adam's Bridge) is used only to fleets of small crafts involved in coastal trading and fishing. Overseas and coastal trading had flourished in this coast over the past years. However, coastal trade was more prominent than the overseas ones. A shipping channel is planned connecting the Gulf of Mannar with the Palk Bay known as the Sethusamudram channel. The idea of Sethu Canal (which passes through Adam's Bridge and the Palk Bay) will transform this into a coast that shall start witnessing fleets of large vessels involved in overseas trading pass by. The structure and function of the Adam's Bridge and the Palk Bay are influenced by the ocean dynamics of the Gulf of Mannar, which is an extension of the Indian Ocean and the Bay of Bengal. The chief seaports on the Gulf of Mannar are Thoothukudi (Tuticorin) in Tamil Nadu, and Colombo in Sri Lanka. While these ports can accommodate deep-draft vessels, the shallow Palk Strait can only accommodate small shallow-draft vessels. In July 2005, the Indian Government took preliminary steps to go ahead with the Sethusamudram Shipping Canal Project, which would create a deep channel linking the Gulf of Mannar to the Bay of Bengal. Project boosters emphasize the benefits of a direct shipping route that connects India's east and west coasts without circumscribing Sri Lanka; environmentalists have warned against the grave damage such a project could cause to the sea life and fisheries of the Palk Strait and the Gulf.

Studies on waves, tides, and currents are minimal for this area and no modeling studies are reported in this area. Hence, the present study will be helpful in identifying the wave characteristics and the variation of wave parameters was attempted. However, Gowthaman et al. (2013) reported the surface wave characteristics around Dhanushkodi based on the measured data in the Gulf of Mannar and in the Palk

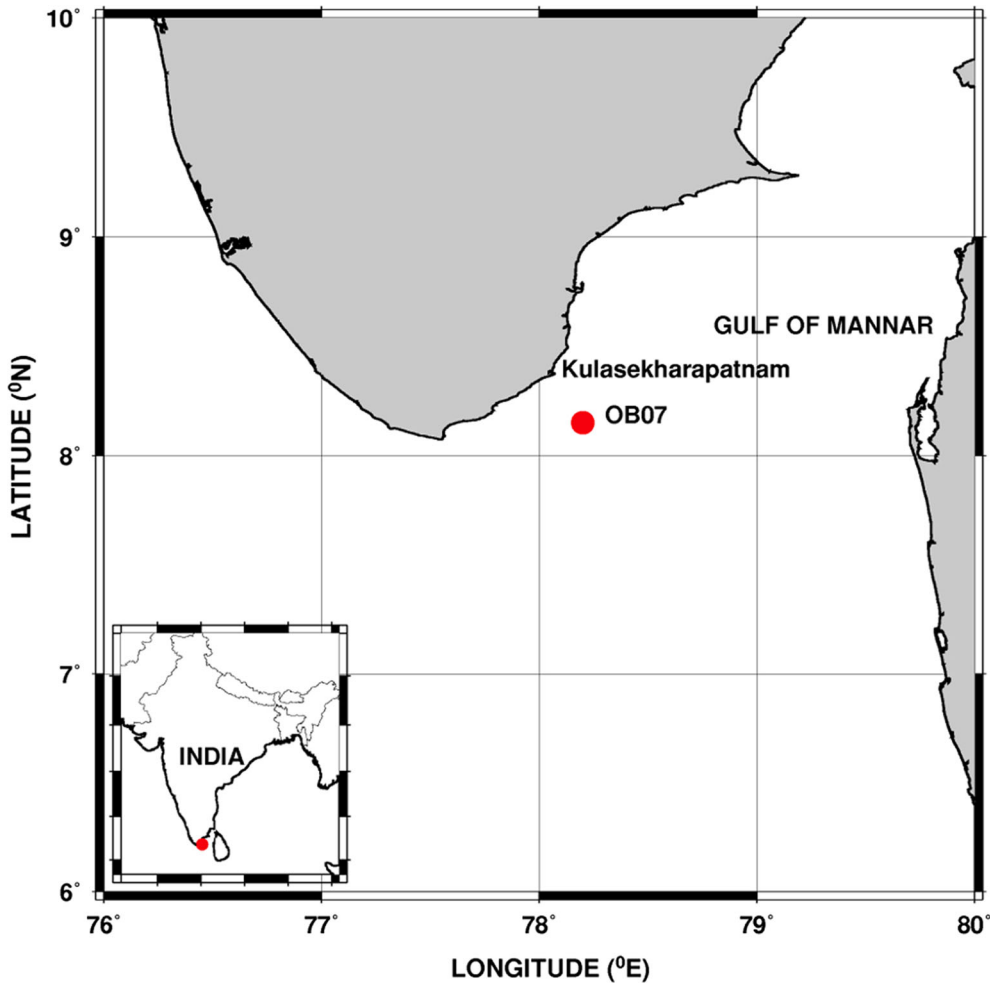

Figure 1
Map showing the study area along with the buoy location (*solid red circle*) in Gulf of Mannar (off Kulasekharapatnam), southeast coast of India

Bay. In another study, Gowthaman et al. (2015) reported on the nearshore waves and Longshore Sediment Transport along the Dhanushkodi coast based on data collected simultaneously in the Gulf of Mannar and Palk Bay using directional wave rider buoys. The objectives of the present study are to identify wave characteristics of the Gulf of Mannar and to predict the significant wave parameters off the Gulf of Mannar. The simulated wave parameters are validated using buoy measurements at the study location. In this piece of work, separate sensitivity simulations are designed using the different parameterizations of the source terms (Generation 3 physics and bottom friction formulation) in the model forced with the blended winds from January 2006 to May 2007. The findings of this study would be useful for modeling/designing the offshore structures or breakwaters off the Periyathalai coast, i.e., beyond the submerged reef to dissipate the wave activity. This study is also essential as wave climate is very important for navigational routes, and hence the location demands many further studies, which will turn out as a helpful navigational aid for the Sethusamudram project.

2. Methods

2.1. Study Location

The offshore region off Kulasekharapatnam, Tamil Nadu (Gulf of Mannar) is the study area (Domain D_2 in Fig. 2) located between Tuticorin and Kanyakumari. Kulasekharapatnam is a coastal fishing village located (8.27°N and Long.78.56°E) along the southeast coast of India between Manapadu and Tiruchendur in Tuticorin District of Tamil Nadu. The village consists of around 1000 families traditionally living and depending on fishing for their livelihood. Similarly, Tiruchendur Manapadu and Periyathalai villages are also important fishermen hamlet located in this region. Periyathalai is located in southern side of Manapadu and about 12 km from Manapadu. An offshore submerged reef that exists at 1 km distance from Periyathalai coast into the sea is hook shaped. The fishermen sailing into the sea for fishing activities are prone to the risk of getting capsized and trapped beneath the submerged reef particularly during rough sea in southwest monsoon. This kind of reef formation is basically by geological processes and formed by calcareous rock. The wave heights of

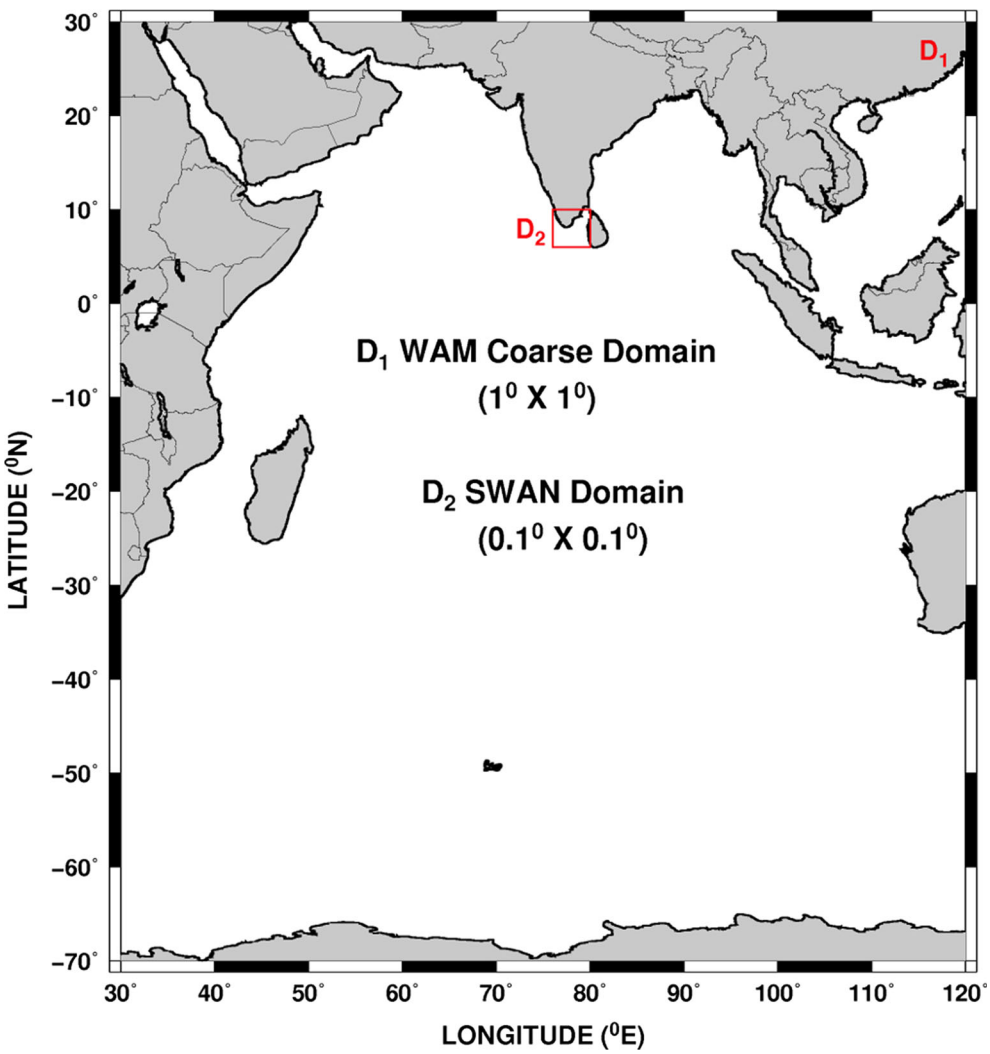

Figure 2
Domains for the numerical experiment (D_1 coarse grid WAM domain and D_2 SWAN domain)

Gulf of Mannar is more during southwest monsoon than northeast monsoon (Gowthaman et al. 2013) and swell waves are predominant in Gulf of Mannar.

During northeast monsoon and fair-weather period, the sea remains relatively calm, resulting which most of the time wave heights is less and the absence of high waves. So fishermen easily sail and cross over the reef without any disturbance and risk. However, during southwest monsoon season, when high waves approach the coastline, they break partly on the reef and propagate further towards the shoreline. The fishing boats crossing over the reef during southwest monsoon are facing problems and risk due to high breaking wave, heavy wind and associated water turbulence in the coastal waters.

According to the local fishermen in Periyathalai village, a small shift in wave direction and approaching angle to the shore will lead to overturn the boat, causing damage to the boat and trapping the fishermen beneath the submerged reef. Further, erosion is a severe problem in this coastal belt. Kulasekharapatnam coastal zone has beach ridges and marine terraces and various stages of these ridges indicate the sea-level fluctuations during the Holocene (Cherian et al. 2012). The rocky promontory located near Kanyakumari plays a pivotal role and provides a "cape effect" by blocking alongshore sediment movement and diverting it offshore (Loveson 1994). Similarly, the submerged reef located off Periyathalai is diverting sediment movement to seaward. Due to this, sediment supply to the northern part of coastal zone is reduced and causing severe beach erosion in Kulasekharapatnam, Manapadu and Tiruchendur coastal areas. The reported tide level in this region are semi-diurnal (Anonymous 2011) with spring tidal range of 0.6 m and neap tidal range of 0.16 m.

2.2. *Data and Methodology*

2.2.1 *Wind Forcing for the Model*

The quality of the wind forcing used to drive a wave model is a critical first-order control upon the wave model outcome. Without high quality wind forcing fields, wave model results may suffer even given the correct physics. Besides, one can theorize that the quality of wind fields turns out to be significantly more basic while considering higher-order wave spectral moments, on the grounds that these terms are all the more specifically connected with shorter waves and subsequently fixing all the more unequivocally to the wind driving.

A high quality surface wind field given by the atmospheric reanalysis (Caires and Sterl 2005; Moeini et al. 2010; Ardhuin et al. 2007) of the ECMWF (European Center for Medium Range Weather Forecasts) known as ERA-Interim (Dee 2011) is utilized in the present work. ERA-Interim is the most recent ECMWF global reanalysis, covering a period from January 1979 to present, with spatial resolutions from 2.5° × 2.5° to 0.25° × 0.25°. Albeit numerous past studies utilizing ECMWF wind information demonstrated that the amplitudes of ECMWF wind were for the most part disparaged (Signell et al. 2005; Cavaleri and Sclavo 2006), estimated waves can be sensible if proper adjustments are made in ECMWF wind information (Mazaheri et al. 2013). In this study, the zonal and meridional components of the ERA-Interim wind in 6 hourly intervals with a spatial resolution of 1° × 1° and 0.25° × 0.25° for the period from January 2006 to May 2007 is chosen to drive the WAM and SWAN models to simulate the waves over southeast coast of India.

To study the sensitivity of the model to different parameterizations at the study location QuikSCAT/NCEP blended winds have been used to force the wave models. QSCAT/NCEP Blended Ocean Winds from Colorado Research Associates (version 5.0) covers from July 1999 to July 2009, with a spatial resolution of 0.5° × 0.5° (latitude × longitude). QuikSCAT/NCEP blended wind products (6-hourly maps) were derived through a spatial blending of the high-resolution scatterometer (QuikSCAT) wind observations with the NCEP/NCAR reanalysis winds (Milliff et al. 1999). The NCEP/NCAR analysis fields are the products of the NCEP Climate Data Assimilation System (CDAS), which was developed for the NCEP/NCAR reanalysis (Kalnay et al. 1996). These data files are available from the NCAR Data Support Section (DSS): DS744.4-QSCAT/NCEP Blended Ocean Winds. In this study, the QuikSCAT/NCEP blended winds (6-hourly) for the period from January 2006 to May 2007 were downloaded and interpolated to 1° × 1° (model grid resolution) for wave hindcasting.

2.2.2 Buoy Data

The National Institute of Ocean Technology (NIOT) had deployed several deep-sea and shallow water moored buoys in the Indian Ocean region (Premkumar et al. 2000) under the National Data Buoy Programme (NDBP) and Indian National Centre for Ocean Information Services, (INCOIS), Hyderabad is designated to share this data with user community. Since 1997, these buoys measure several near surface meteorological and oceanic variables (Venkatesan et al. 2016). The buoy data have proved to be extremely useful in validating reanalysis and satellite products (Sengupta et al. 2001; Senan et al. 2001). The buoy data consists of wind speed and direction at every 3 h intervals. Each 3 hourly wind observations are a 10-min average wind speed and direction sampled at 1 Hz by a cup anemometer with vane installed at 3 m height above the sea level. The accuracy of wind speed measurement is 1.5% of full scale (0–60 m/s), i.e., 0.9 m/s. The sensors used in the measurement of wave parameters are an inertial altitude heading reference system with dynamic linear motion measurement capability. The waves are measured in the buoy by a motion reference unit, which measures absolute roll, pitch, yaw and relative heave. These data are recorded at a rate of 1 Hz for 17 min every 3 h. The significant wave height is estimated as four times the square root of the area under the non-directional wave spectrum. One buoy in the Gulf of Mannar at a depth of 1260 m, southeast coast of India (OB07: 8.27°N, 78.56°E) were selected for the present study and the buoy location is as shown in Fig. 1. The data chosen for the simulation is considered based on the length of data available with minimum gaps during January 2006–May 2007.

2.2.3 Model Description

The details on the wave models used for the present study are as listed as follows.

2.2.3.1 WAM Cycle 4.5.3 The wave model WAM Cycle 4.5.3, is a state-of-art third-generation wave model (WAMDI Group 1988; Gunther and Behren 2011) which is presently operational at ECMWF. The model solves the energy balance equation with exact nonlinear wave–wave interactions for 2D wave spectrum F (f, θ, φ, λ, t), which is a function of frequency f, direction θ, latitude φ, longitude λ, and time t:

$$\frac{\partial F}{\partial T} + \frac{\partial}{\partial \varphi}(\dot{\varphi}\mathrm{F}) + \frac{\partial}{\partial \lambda}(\dot{\lambda}\mathrm{F}) + \frac{\partial}{\partial \theta}(\dot{\theta}\mathrm{F}) = S. \quad (1)$$

Here θ, λ and φ are the rates of change of position and propagation of a wave packet traveling along a great circle path. The source function S is represented as a superposition of the wind input S_{in}, whitecapping dissipation S_{dis}, and nonlinear transfer S_{nl}:

$$S = S_{\mathrm{in}} + S_{\mathrm{dis}} + S_{\mathrm{nl}}. \quad (2)$$

The wave model is capable of predicting ocean wave spectrum. The spectrum has been decomposed into 25 frequency bins and 24 directional bins. The 25 frequency bins of the model range from 0.04 to 0.41 Hz on a logarithmic scale with $\Delta f/f = 0.1$ and direction bins are at 15° resolution. The spatial resolution of the wave model used in this study is 1° × 1° and the integration time step is 20 min.

2.2.3.2 Simulating Waves Nearshore To simulate waves in shallow waters, the SWAN (Simulating Waves Nearshore) model was utilized. Implemented with the wave spectrum method, it is a third-generation wave model that can compute random, short-crested, wind-generated waves in coastal regions as well as in land waters. The SWAN model is used to solve the spectral action balance equation without any prior restriction on the spectrum for the effects of spatial propagation, refraction, reflection, shoaling, generation, dissipation, and nonlinear wave–wave interactions. Information about the sea surface is contained in the wave variance spectrum of energy density $E(\sigma, \theta)$. Wave energy is distributed over frequencies (θ) and propagation directions (σ), where σ is observed in a frame of reference moving with the current velocity, and θ is the direction normal to the wave crest of each spectra component. The expressions for these propagation speeds are taken from linear wave theory (Dingemans 1997), while diffraction is not considered in the model. The action balance equation of the SWAN model in Cartesian coordinates is as follows:

$$\frac{\partial N}{\partial t}+\frac{\partial c_x N}{\partial x}+\frac{\partial c_y N}{\partial y}+\frac{\partial c_\sigma N}{\partial \sigma}+\frac{\partial c_\theta N}{\partial \theta}=\frac{S}{\sigma}, \quad (3)$$

where the right-hand side contains S, which is the source/sink term that represents all physical processes that generate, dissipate, or redistribute wave energy. The equation of S is as follows:

$$S = S_{\text{in}} + S_{\text{ds,w}} + S_{\text{ds,b}} + S_{\text{ds,br}} + S_{\text{nl4}} + S_{\text{nl3}}, \quad (4)$$

where S_{in} is the term for transferring of wind energy to the waves (Komen et al. 1984), $S_{\text{ds,w}}$ is the term for the energy of whitecapping (Komen et al. 1984), $S_{\text{ds,b}}$ is the term for the energy of bottom friction (Hasselmann et al. 1973), and $S_{\text{ds,br}}$ is the sink mechanism term that refers to the energy loss due to depth-induced breaking. The model is available with a variety of physics options, namely Generation 3 (GEN3) for wind input, quadruplet interactions and whitecapping. The different formulations under the GEN3 physics are Komen, Janssen and the Westhuysen option. The major dissipation source term in shallow water within the SWAN model is bottom friction. Intuitively, bottom friction is the dominant form of dissipation in shallow water prior to the onset of depth limited breaking. It may be formulated in three ways within the SWAN model. The Madsen formulation for bottom friction and the Collins formulation for bottom friction are based on the quadratic drag law, while the JONSWAP formulation for bottom friction comes from empirical measurements. In the present study of the sensitivity test, the formulations for bottom friction are compared using the default values for the coefficient of dissipation given in the SWAN model. The default coefficient for the Madsen (Madsen et al. 1988) formulation is 0.05. The default value for the Collins bottom friction (Collins 1972) is 0.015 and 0.038 is the default coefficient for bottom friction in the JONSWAP formulation (Hasselmann et al. 1973).

2.2.3.3 Model Set Up and Initialization The integrated model of WAM (Cycle 4.5.3) and SWAN is utilized to simulate the waves in the study area. In this study, two different model domains were used, as shown in Fig. 2, to accommodate the swells from the southern ocean. The outer domain is (D_1) a finite difference coarse grid extending from 30°E to 120°E and 70°S to 30°N, and the simulation studies were performed using WAM Cycle 4.5.3 (Gunther and Behren 2011). For better representation of the wave spectra distribution, the model uses 25 frequencies ranging from 0.04177 to 0.41145 Hz and 12 directions with constant increment. Source integration and propagation time steps were set to 10 and 20 min, respectively. The boundary conditions containing information of the 2D wave energy spectra from coarse grid (Domain D_1) were nested to the finite difference grid domain D_2 (76°E–80°E and 6°N–10°N) which is the region of study. The SWAN model was used to predict the wave characteristics in the domain D_2 (Fig. 2) using the boundary conditions from D_1. The number of bins in the frequency and directional space are 50 and 36, respectively, which essentially takes care of frequency space in the surface gravity wave spectrum. The frequency used in SWAN ranges between 0.05 and 0.5 Hz. Model simulations were executed in a nonstationary mode with a computational time step of 30 min. The nesting of WAM model to SWAN enables the free propagation of low frequency swells into the study region. The model was forced with the 6 h ECMWF ERA-Interim and QuikSCAT/NCEP blended winds of 1° × 1° and 0.25° × 0.25° for the domain D_1 and D_2, respectively. The bathymetry data used is the ETOPO2 database.

3. Results and Discussion

In this section, we will introduce the validation results obtained for the wind utilized for driving the model and for the significant wave parameters and finally concluding the deep water wave characteristics of Gulf of Mannar. The acquired wave data from the deep water buoy for the period from January 2006 to May 2007 was investigated and the seasonal variation of wave attributes were inspected. Different statistical measures, such as mean error (bias), root mean square error (RMSE), scatter index (SI), and Pearson correlation coefficient (R) are utilized to assess the quality of wind forcing and wave model performance by comparing with the corresponding buoy observations, computed as,

$$\text{Bias} = \frac{1}{n}\sum (M_i - B_i), \quad (5)$$

$$\mathrm{RMSE} = \frac{1}{n}\sqrt{\sum (M_i - B_i)^2}, \tag{6}$$

$$\mathrm{SI} = \frac{\mathrm{RMSE}}{\bar{B}}, \tag{7}$$

$$R = \frac{\sum (M_i - \bar{M})(B_i - \bar{B})}{\sqrt{\sum (B_i - \bar{B})^2}\sqrt{(M_i - \bar{M})^2}}, \tag{8}$$

where B_i and M_i indicate the buoy measure and wind forcing/modeled wave parameters, respectively; $\bar{B}$ and $\bar{M}$ are their corresponding mean values and n is the number of observations used for the comparison. Wave power is calculated using wave power equation (Pond and Pickard 1991) to estimate the strength of the wave, and the wave steepness was used to classify the sea and swell during all months and different seasons.

3.1. Wind Validation

The quality of simulated wave heights depends essentially on the precision of the wind fields utilized. The wave heights roughly scale with the square of wind speed and this infers that an error of around 10% in the driving wind fields will bring about an error of at least 20% in the hindcast wave height (Pillar et al. 2008). To evaluate the quality of wind forcing, an attempt is made to compare the ECMWF ERA-Interim winds with the observations from NDBP buoys. The comparison amongst ECMWF ERA-Interim and buoy data was performed for one location (OB07) off Kulasekharapatnam, Gulf of Mannar.

The ECMWF ERA-Interim wind speeds demonstrated good agreement with buoy measured wind speeds in the Gulf of Mannar, southeast coast of India as apparent in the time series plots (Fig. 3). From the time series plots, it is clear that the ECMWF ERA-Interim winds do not have appreciable bias with respect to observations at buoy locations. The detailed statistics of the validation is presented in Table 1. The average wind speed and standard deviations demonstrates almost the same range as buoy observations at the study area. However, standard deviations uncover that the ECMWF ERA-Interim wind speeds are more scattered as compared with buoy measured wind speeds. A high correlation coefficient of 0.97 and RMSE of 0.74 indicate a good match between buoy and model winds. The high correlation coefficients recommend that both measured and ECMWF ERA-Interim winds follow a similar annual pattern.

To determine the characteristics of the directionality variability along with their magnitudes, the rose plots for both observation and wind forcing are plotted. Seasonal directional variability of wind along with their magnitudes is elusive and the same can be observed for every one of the seasons from the rose plots (Fig. 4). The rose plots uncover that the buoy measured seasonal distribution of the winds and their directional variability with respect to seasons are well represented in the ECMWF ERA-Interim winds too. Further, the mismatches in the rose plot may be due to the model inefficiency in predicting the directions.

3.2. Model Validation

Comparison of the wave model forecasts with observations is essential to characterize model deficiencies and identify areas for improvement. Based on the availability of buoy data in the study period, a comparison is made between buoy and model derived wave heights at one location in the Gulf of Mannar, southeast coast of India (OB07) from January 2006 to May 2007. To evaluate the model performance, model simulated significant wave height, mean wave direction and mean wave period are compared with the buoy observations. The comparisons show that the model derived wave parameters agree well with the observed wave parameters as shown in Fig. 5. Quantitatively, the model output obtained here are consistent with those obtained at the buoy location.

It is observed that the model could reproduce the variability in wave heights at that buoy location. The overall trend in wave heights shows a reasonable good match with buoy observations. The simulated mean wave period shows a constant negative bias throughout the simulation period with a higher discrepancy in the months of April, November, and December. One conspicuous feature from the comparison of mean wave direction is that, the model could simulate the observed direction well irrespective of the seasons. Figure 5c reveals that waves prevail from south-southwest (SSW) direction from

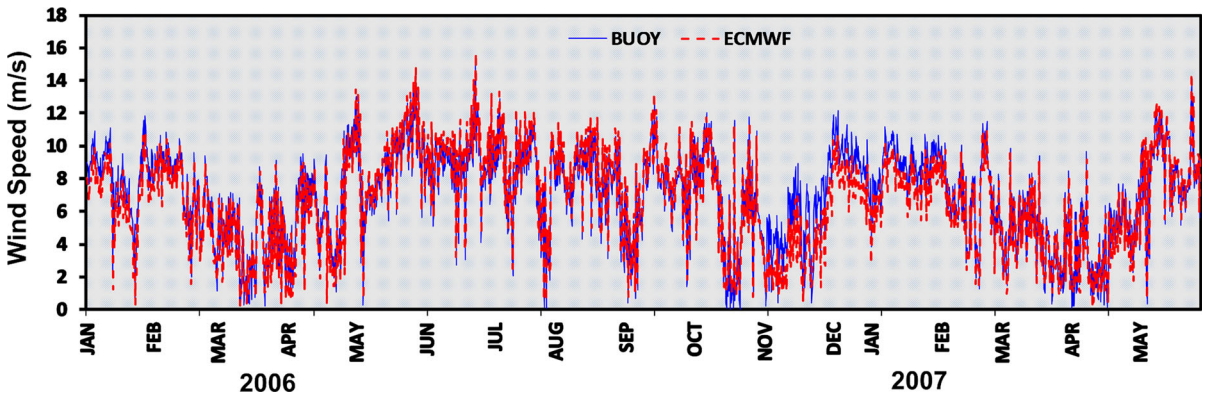

Figure 3
Time series plot of buoy and ECMWF ERA-Interim wind speeds at location OB07

Table 1

The statistics of the comparison between buoy and ECMWF ERA-Interim wind speeds

Buoy location	Average (m/s)		Standard deviation (m/s)		Bias (m/s)	RMSE (m/s)	Correlation
	Buoy	ECMWF ERA-Interim	Buoy	ECMWF ERA-Interim			
OB07	6.97	6.72	2.85	2.94	−0.36	0.74	0.97

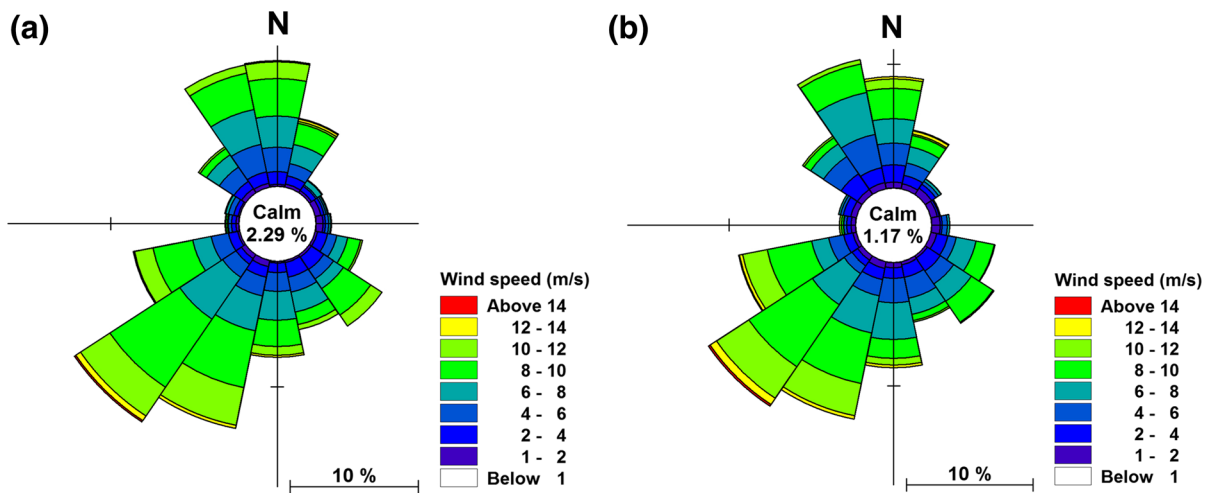

Figure 4
Directional histograms of wind speeds, comparing **a** measured and **b** ECMWF ERA-Interim winds at buoy location OB07

April to October. However, the wave pattern shifts towards the east-southeast (ESE) direction during November and from NE direction during December as influenced by the NE monsoon winds. The wave direction is highly variable during monsoon and post-monsoon season. Gowthaman et al. (2013) reported that wave direction is highly variable during January and May at Gulf of Mannar, however, in the present

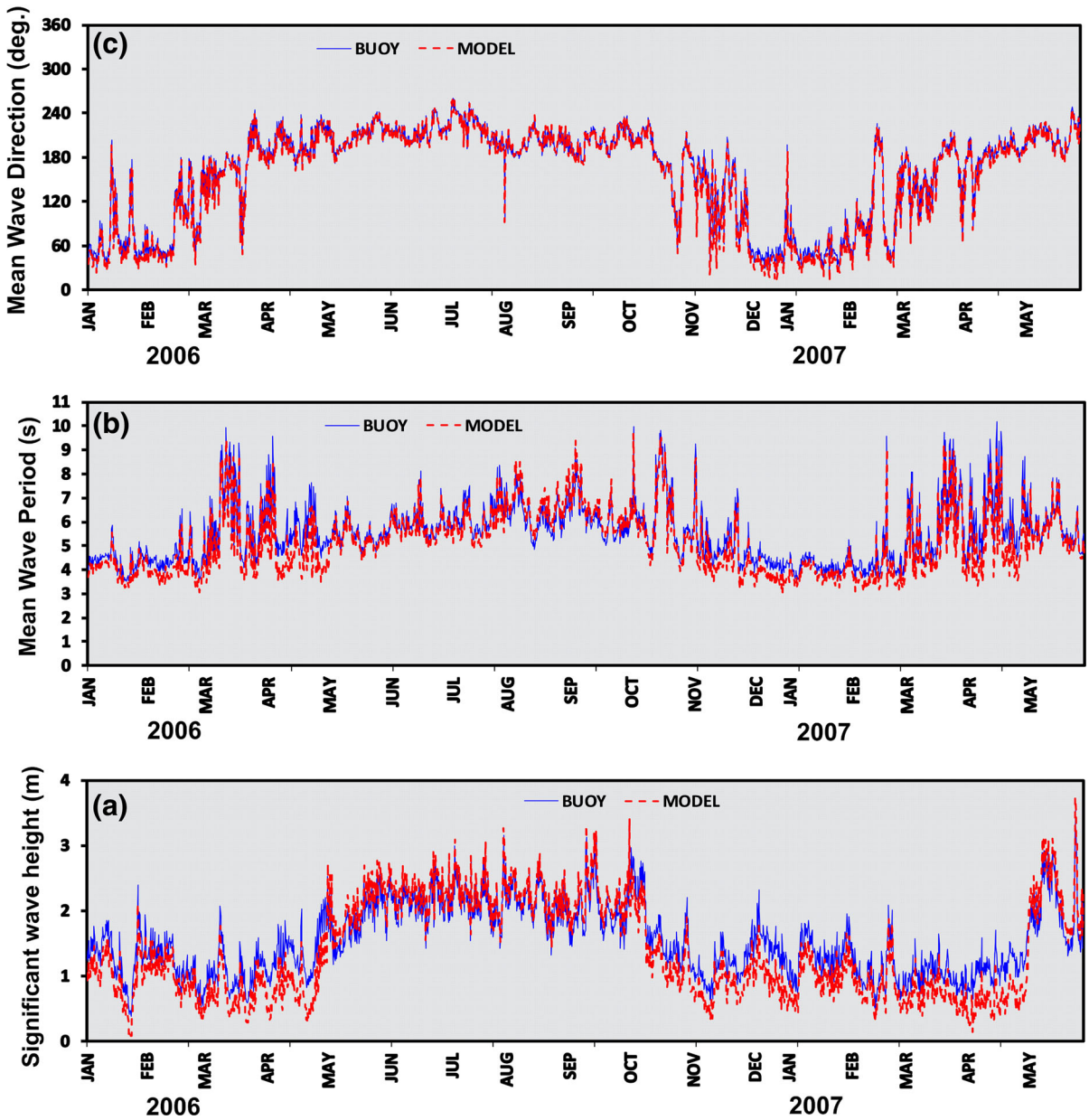

Figure 5
Time series plots of buoy and model simulated wave parameters at location OB07 **a** significant wave height, **b** mean wave period and **c** mean wave direction

study, a variable wave direction was noticed during post-monsoon season and also during NE monsoon (Fig. 5c).

A detailed statistics of the validation is presented in Table 2. The model simulated wave parameters agree reasonably well with the observations. As observed in the winds, the buoy-measured wave parameters are more scattered as compared to model simulated parameters. A general feature noticed from these results is that there is definite indication of different performance of the model during the different seasons. The results are consistently better

when the meteorological conditions are more defined and winds are stronger, viz. southwest monsoon as shown in Table 3.

Table 3 shows the overall seasonal scale performance of model computed significant wave heights and mean wave period with buoy observations. Various statistical measures such as bias, RMSE, SI and R are examined to evaluate the model performance. A strong positive correlation ($R > 0.8$) between buoy and model wave height is noticed during pre- and southwest monsoon (SWM) season. The correlation coefficients for the other two seasons are 0.76 (post-monsoon) and 0.71 [northeast monsoon (NEM)], which are reasonably good. A positive bias is observed for pre- and southwest monsoon which signifies that model computed wave heights are slightly higher in comparison with buoy observations. The RMSE for wave height comparisons varied from 0.13 to 0.38 which implies a good fit. The lower values of SI also indicate a good fit between model and measured significant wave height. Similarly, the comparisons of mean wave period for all seasons were reasonably good with the highest correlation for southwest monsoon ($R = 0.97$) and lowest for northeast monsoon ($R = 0.72$). The overall evaluation based on statistical measures show that the model performs well during all seasons and the best performance being exhibited in the southwest monsoon period.

The seasonal directional variability of waves along with their magnitudes can be assessed using the rose plots as shown in Fig. 6. The overall comparison shows similar wave pattern for both the measured and modeled data. It is observed that only 0.31% of the buoy measured wave heights are below 0.5 m; but 6.63% represents less than 0.5 m waves in simulated waves. This gives an insight to the overestimation of the low wave heights in the buoy. Comparing the seasonal distribution of waves, during southwest monsoon the directions are very similar, with the main direction of wave incidence being from the southwest. The model slightly underestimates the occurrence of higher waves from all directions and this underestimation is possibly linked with the directional discrepancy linked with the wind forcing as seen in the directional histograms of the wind. These comparisons, although qualitative, show that the overall wave characteristics are well represented by the model for the period compared at the buoy location OB07.

3.3. *Sensitivity to Changes in the Parameterization of the Source Terms*

Accuracy of the wave model results is governed by forcing fields, source term parameterizations and effect of numerics. The SWAN model has many parameters that may be adjusted by the modeler. The purpose of this sensitivity study is to determine which SWAN model parameters produce significant change in the wave characteristics over the study area. This will also provide insight into, which parameters must be varied to produce a physically accurate model and model results that agree well with observed wave characteristics.

Different parametrizations of the source terms are included in SWAN model. Two suites of model tests were performed to measure the sensitivity of SWAN to several of these parameters. In this study, we will consider the parameterization of two of the source terms, namely GEN3 Physics and bottom friction. These terms are very important in the spectral evolution (Ris 1997) of significant wave parameters. In the analysis, following we use the defaults of the

Table 2

The statistics of the comparison between buoy and simulated wave parameters (January 2006 to May 2007)

Parameters	Average		Standard deviation (m/s)		Bias	RMSE	Scatter index	Correlation
	Buoy	Model	Buoy	Model				
Significant wave height (m)	1.53	1.37	0.53	0.72	−0.18	0.29	0.19	0.97
Mean wave period (s)	5.50	5.13	1.20	1.29	−0.46	0.51	0.09	0.95

Table 3

Validation statistics between model and buoy observations for different seasons

Seasons	Average		Standard deviation (m/s)		Bias (m)	RMSE (m)	Scatter index	Correlation
	Buoy	Model	Buoy	Model				
(a) Significant wave height								
Pre-monsoon	1.60	1.44	0.51	0.80	0.01	0.38	0.24	0.84
SWM	2.10	2.23	0.31	0.30	0.02	0.13	0.06	0.95
Post-monsoon	1.44	1.14	0.49	0.49	−0.001	0.30	0.21	0.76
NEM	1.18	0.89	0.32	0.31	−0.003	0.29	0.25	0.71
(b) Mean wave period								
Pre-monsoon	5.79	5.19	0.98	0.98	−0.03	0.73	0.12	0.89
SWM	6.17	6.21	0.70	0.78	0.01	0.33	0.05	0.97
Post-monsoon	5.68	5.24	1.33	1.40	−0.002	0.47	0.08	0.85
NEM	4.85	4.41	1.21	1.19	−0.001	0.45	0.09	0.72

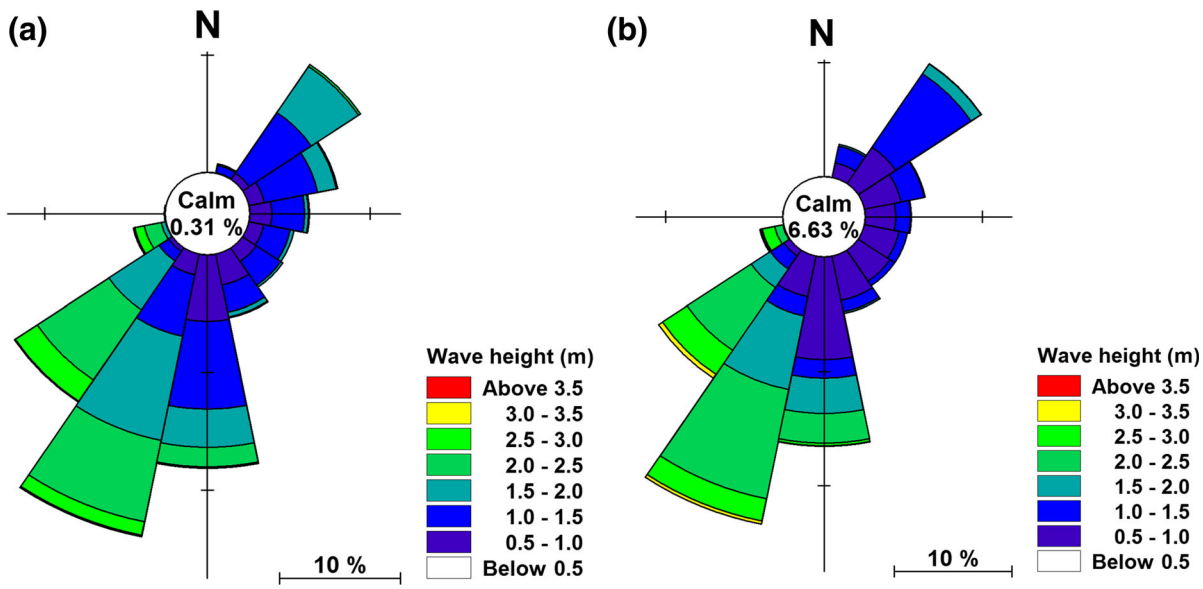

Figure 6
Directional histograms of wave heights, comparing **a** measured and **b** modeled data at buoy location OB07

SWAN model (the Komen parameterization for the GEN3 physics and the JONSWAP parameterization for the bottom friction term). This will be considered as the default case in this study and in the rest of the cases to be tested, we will only change simultaneously one of the default parameters to test the sensitivity of the model, with all other physical conditions remaining the same. Results from these experiments have been compared with the OB07 buoy data off Kulasekharapatnam.

In a sensitivity study, choice of wind input is critical control on the wave model outputs. Hence, the SWAN model has been forced with the best available blended wind fields (QuikSCAT/NCEP, 6 hourly) to study the model sensitivity using the GEN3 physics and bottom friction formulations. Figure 7 shows the comparison of simulated significant wave parameters between the results of GEN3 parametrization, namely Komen, Janssen and Westhuysen, with the buoy data off the Gulf of

Mannar. Figure 7a shows the comparison of model simulated wave heights using Komen, Janssen and Westhuysen options with the buoy data. Table 4 shows the statistics of the comparison of significant wave parameters based on different GEN3 physics options. The Janssen formulation produced significantly better results in wave height than the default Komen formulation. As seen in figure, the correlation between buoy and simulated wave heights is higher in the case of Janssen ($R = 0.98$) than in the case of Komen ($R = 0.89$) and Westhuysen ($R = 0.86$), implying much better agreement with buoy data for model simulation with Janssen option. Root mean square error (RMSE) between simulated wave height and buoy wave height for the period from January 2006 to May 2007 (Fig. 7a) shows that the simulations using Janssen option captures the wave heights with better accuracies during the entire year as compared to other two options.

During the monsoon phase, however, there is improvement in the performance of Komen physics. The bias is negative using Komen physics ($B = -0.29$) indicating an under prediction and Westhuysen physics option highly over predicts the simulated wave heights at the study location. It is also noted that during the monsoon season both Komen and Janssen physics options follows the buoy signals with good accuracies. The differences in the simulations of these physics options can be primarily attributed to the difference in the parameterization of the whitecapping processes along with the exponential growth of the waves due to wind inputs. The study area of the tropical Indian Ocean is dominated by the easterly trade winds throughout the year except in the monsoon months. The rapidly changing velocity of easterly winds causes the shorter fetch over the ocean in almost all the months. However, during the monsoon the differential heating of the

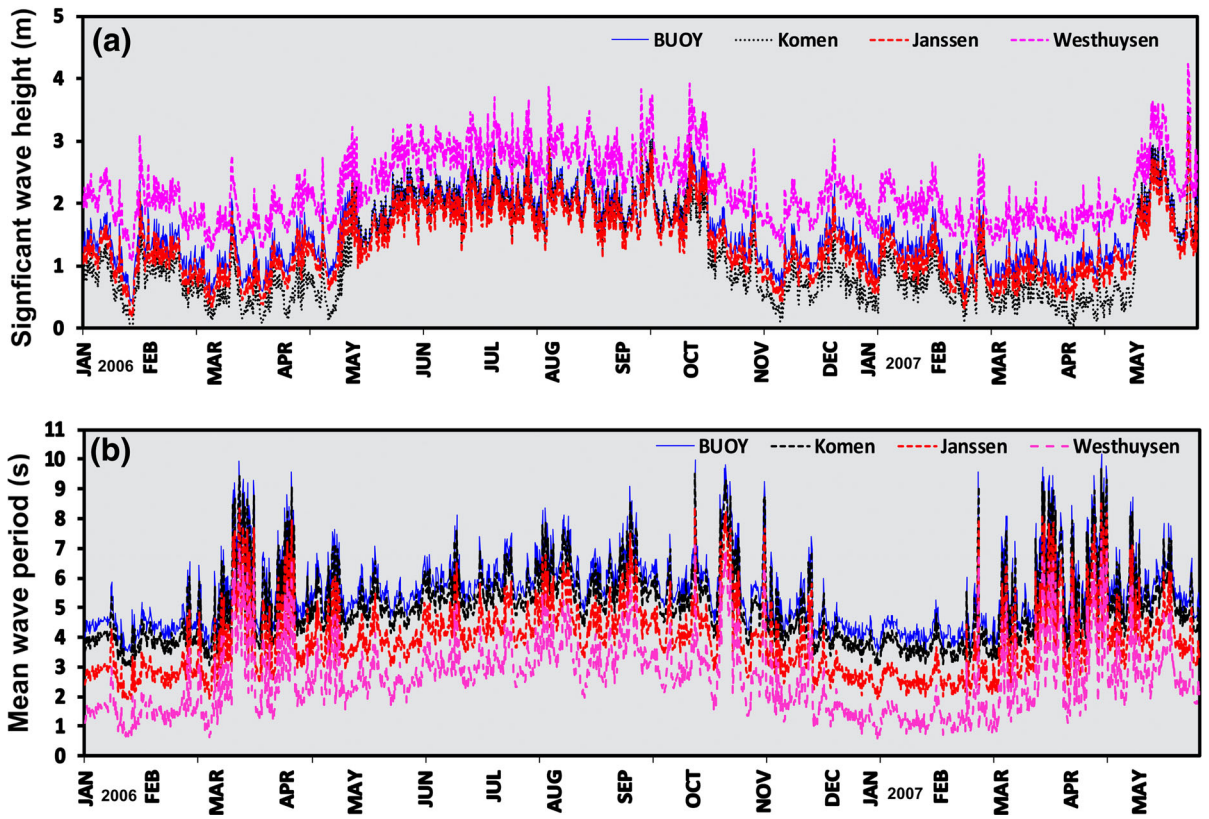

Figure 7
Sensitivity to wind parameterization: variation of **a** significant wave height and **b** mean wave period using GEN3 physics option in SWAN model with buoy data

Table 4

Statistics for significant wave parameters based on GEN3 physics in SWAN compared to measurements from buoy off Kulasekharapatnam

Formulation	Bias	Correlation coefficient	RMSE	Scatter index
(a) Significant wave height (m)				
Kome	−0.29	0.89	0.43	0.28
Janssen	0.06	0.98	0.21	0.13
Westhuysen	0.31	0.86	0.48	0.45
(b) Mean wave period (s)				
Komen	0.08	0.95	0.52	0.09
Janssen	−0.19	0.87	1.63	0.29
Westhuysen	−0.32	0.83	2.91	0.53

land mass and ocean causes the temperature gradient that sets up the persistent cross-equatorial flow of westerly over the Indian Ocean. This causes a rough sea state with the enhancement of wave growth, resulting in steeper waves under the influence of wind. Thus, the Indian Ocean is marked by large fetches with persistent wind velocity during the monsoon period of June to September while in other months of the year; it has shorter fetches with rapid changes in wind velocity over the ocean surface.

Throughout the year, the Komen option shows underestimation of wave height, whereas in the monsoon period it is able to simulate more realistically compared to other months. The Janssen formulation applies a different method for determining whitecapping dissipation than the Komen formulation. The Janssen option considers the dissipation of the high frequency waves more rapidly than that of low frequency waves, making much more realistic estimates of wave height with much lower SI (0.13) than Komen (SI = 0.28) and Westhuysen (SI = 0.45) throughout the year even in the monsoon season. The B, R, RMSE and SI values between simulated and buoy wave heights for the period from January 2006 to May 2007 indicates that the model with Janssen simulation performs much better than the other two GEN3 physics options (Table 4).

The performance of different simulations using GEN3 physics options has been evaluated for mean wave period (Fig. 7b) by comparing with in situ buoy data off Kulasekharapatnam. The comparison (Table 4) of mean wave period with Komen option shows a higher degree of accuracy ($R = 0.95$) as compared with Janssen ($R = 0.87$) and Westhuysen (0.83) physics option. Both Janssen ($B = -0.19$) and Westhuysen ($B = -0.32$) options have under predicted the mean wave period indicating a negative bias. It is observed that at the study area both Janssen and Westhuysen options show very high RMSE (1.63 and 2.91) and SI (0.29 and 0.53), indicating Komen as the best option in simulating wave periods at the study location.

The term due to bottom friction is a dominant mechanism, which becomes important in shallow waters for dissipation of wave energy in the SWAN model. It can be formulated by means of three different parametrizations (the empiric model based on the JONSWAP experiment, the Collins model and the Madsen one) which uses slightly different mechanisms to calculate dissipation. The formulations produce varying results in this study.

Figure 8a shows the comparison of model simulated wave heights using JONSWAP, Collins and Madsen options with the buoy data. Table 5 shows the statistics of the comparison of significant wave parameters based on different bottom friction options. As seen in figure, the correlation between buoy and simulated wave heights is higher in the case of JONSWAP option ($R = 0.96$) than in the case of Collins ($R = 0.87$) and Madsen ($R = 0.74$), implying much better agreement with buoy data for model simulation with JONSWAP option. Although slight underestimation is noted using JONSWAP, the model performs well in the monsoon season. The very low bias ($B = 0.08$), RMSE = 0.35 and SI = 0.23 between simulated and buoy wave height for the period from January 2006 to May 2007 (Fig. 7a) shows that the simulations using JONSWAP option

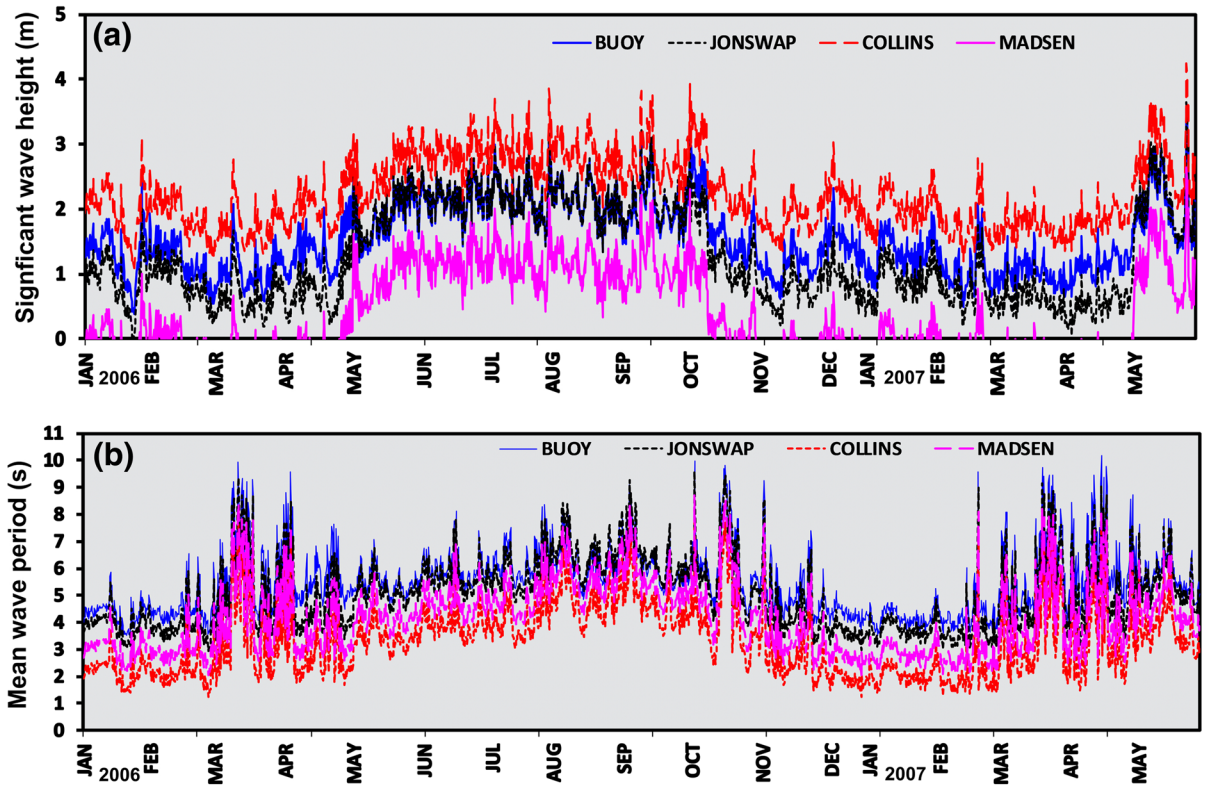

Figure 8
Sensitivity to bottom friction parameterization: variation of **a** significant wave height **b** mean wave period using different bottom friction formulations in SWAN model with buoy data

Table 5

Statistics for significant wave parameters based on different bottom friction formulation in SWAN compared to measurements from buoy off Kulasekharapatnam

Formulation	Bias	Correlation coefficient	RMSE	Scatter index
(a) Significant wave height (m)				
JONSWAP	0.08	0.96	0.35	0.23
Collins	0.39	0.87	0.61	0.46
Madsen	−0.36	0.74	0.83	0.65
(b) Mean wave period (s)				
JONSWAP	0.13	0.96	0.59	0.17
Collins	−0.29	0.89	2.19	0.39
Madsen	−0.16	0.92	1.41	0.25

captures the wave heights with better accuracies during the entire year as compared to other two formulations.

The Collins formulation shows over prediction for wave heights at the study area with $B = 0.39$ and RMSE = 0.61, while the Madsen formulation under predicts highly with very high RMSE = 0.83 and SI = 0.65 (Table 5). The mean wave period (Fig. 8b) also shows best results with JONSWAP option ($R = 0.96$) with slight underestimation, but at the same time it shows contrasting results using other two formulations. The Collins and Madsen formulation

are under predicting the mean wave periods throughout the year with better performance exhibited by Madsen formulation. It is also noted that both Collins and Madsen formulations gave very high RMSE 2.19 and 1.41, respectively, at the study area. The JONSWAP and Madsen formulations show better performances during the monsoon season for mean wave period. The differences in the simulations of these bottom friction options can be primarily attributed to the difference in the mechanisms. The JONSWAP formulation for bottom friction was determined empirically for swell waves in the North Sea and assumes a constant bottom velocity, and hence this approximation gives good results. In contrast, the Collins formulation depends on as implied form of the quadratic drag law using wave-induced bottom velocity, where dissipation is determined from bottom velocity and a drag coefficient determined experimentally. The Madsen formulation for bottom friction is more dissipative than the other two formulations and uses quadratic drag law, where the friction factor depends on a value for bottom roughness and local bottom velocity.

Thus, the sensitivity study dictates that the Janssen and Komen physics follows the experimental signal with better accuracy for wave height and wave period. Similarly, the JONSWAP formulations give the best results for bottom friction for both height and period at the study location, and hence the applicability of the model with the desired parameterizations at the study location is justified.

3.4. Sea State and Wave Characteristics

Wave data collected during January 2006–May 2011 is used to analyze monthly, seasonal and annual wave characteristics of deep water waves. Significant wave height varied between a minimum of 0.4 and a maximum of 3.8 m during January 2006–May 2007 (Fig. 9). The observed wave period for the study area was found to be in the range between 3.4 and 10.1 s, and a mean period of 5.5 s was observed. The significant wave height (H_s), wave direction and wave period variations during the study are presented in Fig. 5. The observed significant wave height (H_s) shows an increasing trend from January 2006 to May 2007, and minimum (0.4 m) and maximum height (3.8 m) were observed during post-monsoon (January) and pre-monsoon (May), respectively. It is observed from the measured time series data at the study location that H_{max} varied from 0.64 to 6.22 m with mean value of 2.53 m in the study area. Wave activity is high during southwest monsoon in the month of September for 2006 and wave activity was low during post-monsoon season (January to March 2006) and a maximum wave height of 3.8 m was recorded during May 2007.

The study by Gowthaman et al. (2013) has reported 5.4 m as a maximum wave height (H_{max}) in Dhanushkodi region of Gulf of Mannar with a mean value of 1.4 m. The significant wave height varied from 0.2 to 2.7 m with mean value of 0.9 m (Gowthaman et al. 2013). However, maximum wave height (6.22 m) was noticed in the present study (OB07 location) off Kulasekharapatnam. At Kulasekharapatnam, the waves are from south-southwest. The wave directions prevailed from 19° to 264° for the period of study and it mostly varied 94–264° during SW monsoon and 65–238° during NE monsoon.

A number of parameters that define the wave field which a structure has to withstand are needed in the designing of a structure in offshore region. A designer often needs the relationship between significant wave height and mean wave period. In Fig. 10a, we show this relationship as revealed by the observations reported in this paper. The correlation is moderate (0.71) due to the presence of wind seas and swells. The mean wave period varies between 3 and 10 s with mean value of 4 s. Similarly, the variation of wave height with wave period for different seasons was examined and shown in Fig. 11. There is no appreciable correlation as is evident from the scatter plots for pre-monsoon (Fig. 11a), post-monsoon (Fig. 11c) and northeast monsoon (Fig. 11d). But the southwest monsoon period showed fairly good correlation of 0.78. Scatter plot of wave power per unit width against mean wave direction (Fig. 10b) indicates that high wave power (>10 kW/m) was from southwesterly waves (190°–240°) and occurred during the southwest monsoon period. During other periods, the wave power was less than 10 kW/m.

To better understand the variation of significant wave height and mean wave period within a specified

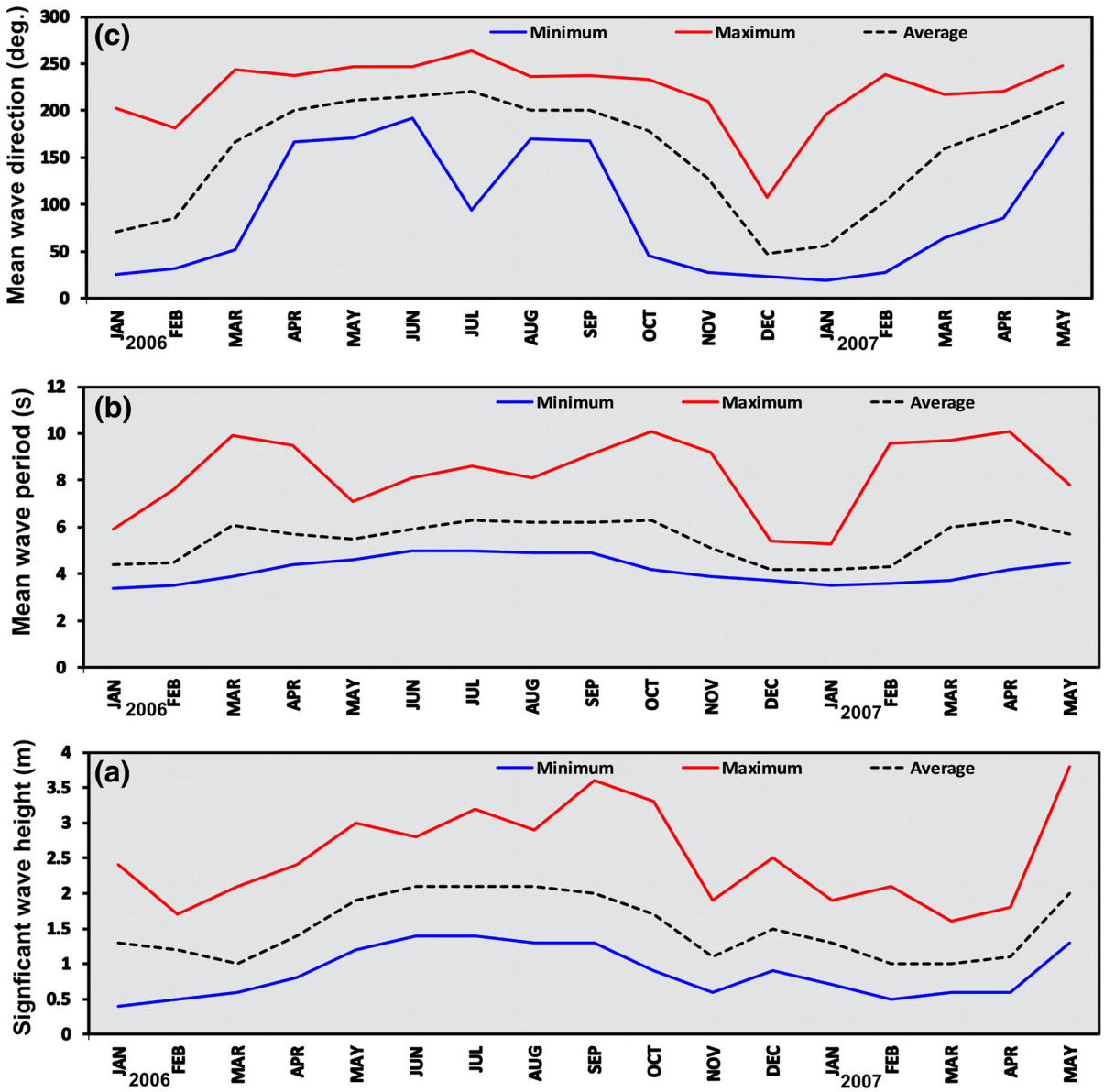

Figure 9
Monthly variation of sea state variables from January 2006 to May 2007

range of values, the probability density function was plotted to analyze the overall distribution during January 2006–May 2007. A probability histogram is the simplest way to represent its distribution graphically, where the area of the rectangles equal their corresponding probabilities. Figure 12 provides the distribution of significant wave height (Fig. 12a) and mean wave period (Fig. 12b) for the study location along with the best fit lognormal/normal distribution. The *X*-axis denotes the significant wave height and mean wave period in seconds and the *Y*-axis shows the height of the histograms, and for the best fit curves it denotes their corresponding probability. The solid thick blue lines show the best fit distribution for the period having 95% confidence level of significance.

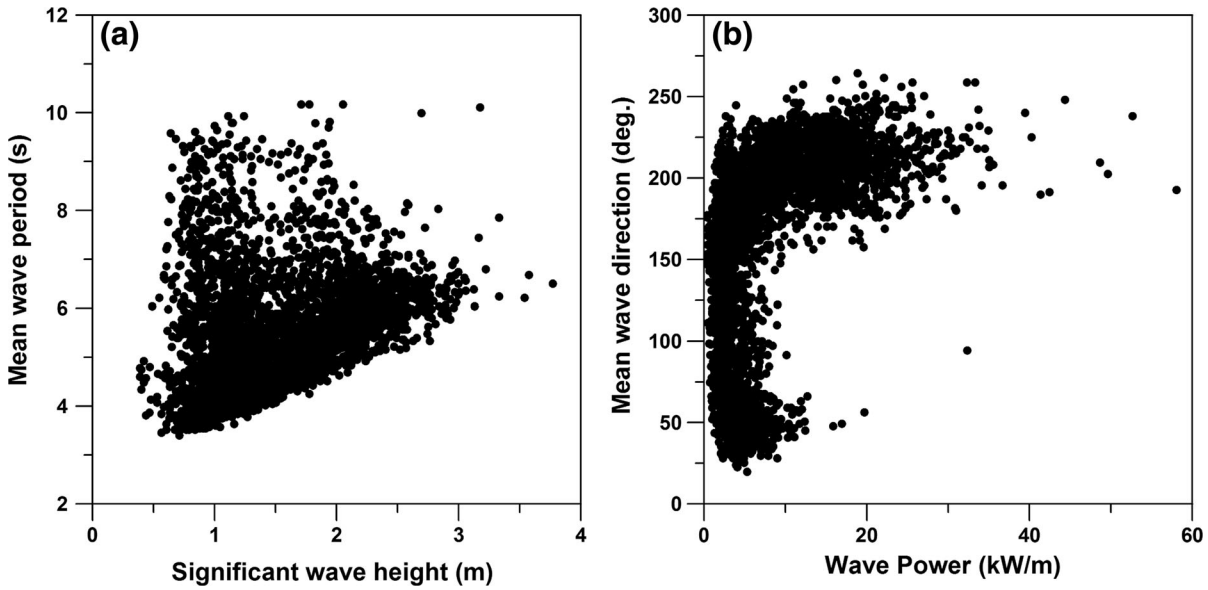

Figure 10
Scatter plot variation of **a** significant wave height with mean wave period and **b** mean wave direction against wave power from January 2006 to May 2007

The most probable significant wave heights vary in the range between 0.8 and 1.2 m for the period of study, and mean wave period shows a probability of 4–5.6 s. In the case of measured waves (Fig. 12a), 95% of the time the significant wave height is less than 2.48 m. The number of events with wave heights more than 1 m is around 25%. It is also observed that 25% of the waves were with wave period more than 4.54 s, whereas 95% of the waves were with wave period more than 7.85 s. In an engineering perspective, the trends observed in significant wave height needs to be accounted during the design stage and procedural planning for coastal and offshore structures. The nature of sea state is also identified based on the wave steepness (H_{m0}/L). The wave steepness is expressed as the ratio between the significant wave height and the wave length ($L = 1.56T^2$), where T is the mean wave period of the peak period. The wind sea and swell are classified to understand the dominant wave pattern in the study area.

Thompson et al. (1984) classified ocean waves based on (H_{m0}/L) as sea, young swell, mature swell and old swell. According to their classification, locally generated waves or sea waves have steepness values greater than 0.025. Similarly, steepness less than 0.025 can be referred as swells. The swells are further classified as: old swells ($H_{m0}/L < 0.004$), mature swells ($0.004 \leq H_{m0}/L < 0.01$) and young swells ($0.01 \leq H_{m0}/L < 0.025$). The present study also examined the sea and swell characteristics at the study area using the wave steepness. Figure 13 shows the percentage of dominance of swells and seas for the different month of the study period. The percentage dominance of seas and swell for the study period from January 2006 to May 2007 is 75.9 and 24.0%, respectively. The study shows that swells are predominant during non-monsoon (January–April), and during rest of the year, wind Sea dominates (Fig. 13). Even though wind seas are predominant during May–December; the role of swell is also significant. Dominance of swell is maximum (69.4%) during April and dominance of wind sea is maximum (100%) during December. The seasonal dominance of sea showed a maximum during southwest monsoon (87.1%) and swell was maximum during post-monsoon (32.8%). It is also noted that during pre-monsoon and northeast monsoon the wind sea dominance was high (70 and 75.5%, respectively). Hence, the analysis clearly indicates the dominance of wind seas off Kulasekharapatnam during January 2006–May 2009.

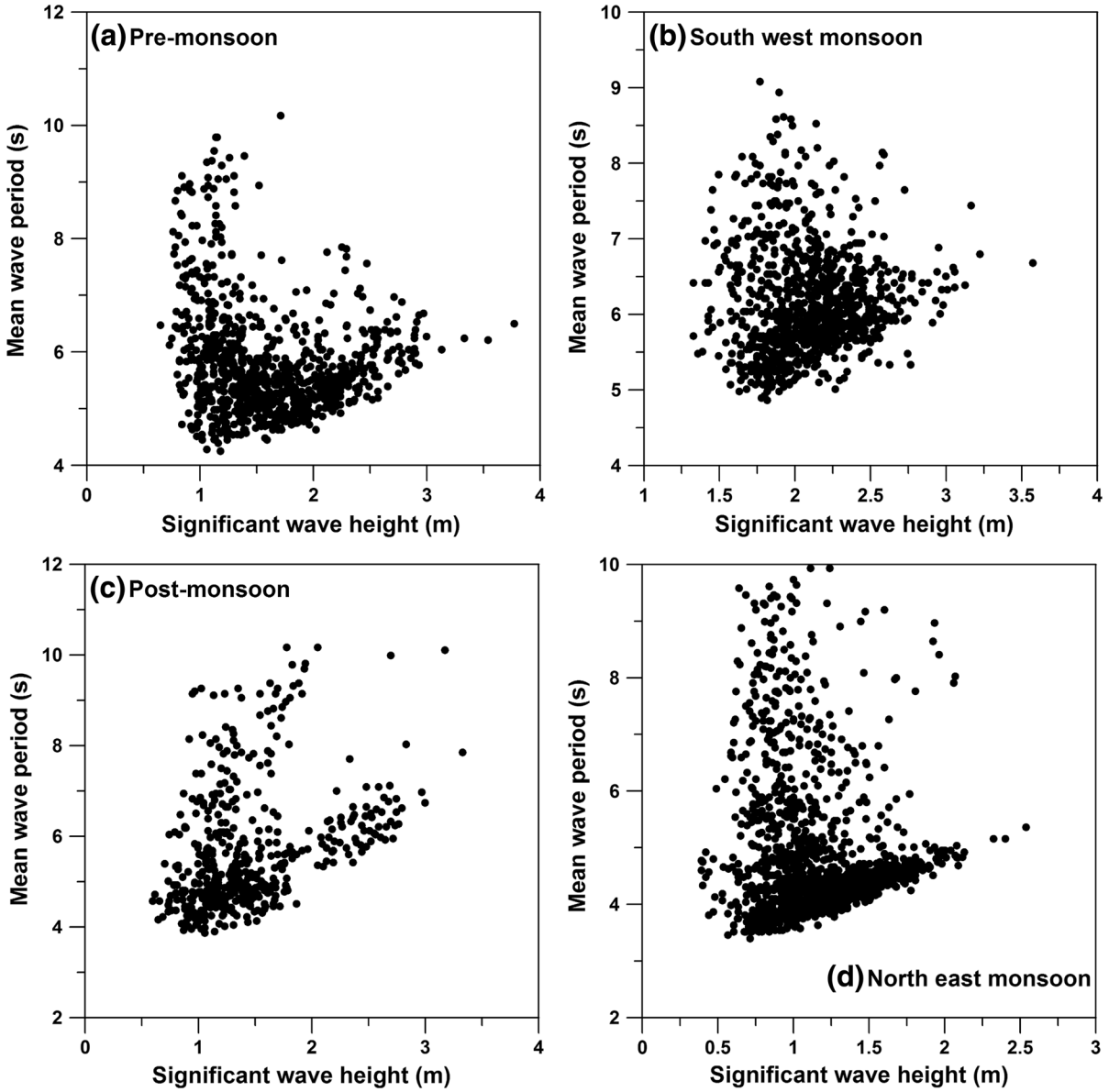

Figure 11
Variation of mean wave period with significant wave height during four different seasons: **a** pre-monsoon, **b** southwest monsoon, **c** post-monsoon and **d** northeast monsoon

4. Conclusions

The study provides an investigation and analysis on the wave characteristics over the region off Kulasekharapatnam. The study has potential practical value to comprehend the characteristics of wind-waves having direct ramifications along the coastal zone and deep water applications, and consequently it can be a good reference for the upcoming projects for navigation. The inferences acquired from this study are based on a comprehensive analysis of the measured data and modeling studies for the period from January 2006 to May 2007 off Kulasekharapatnam. The buoy data obtained at the study location provided

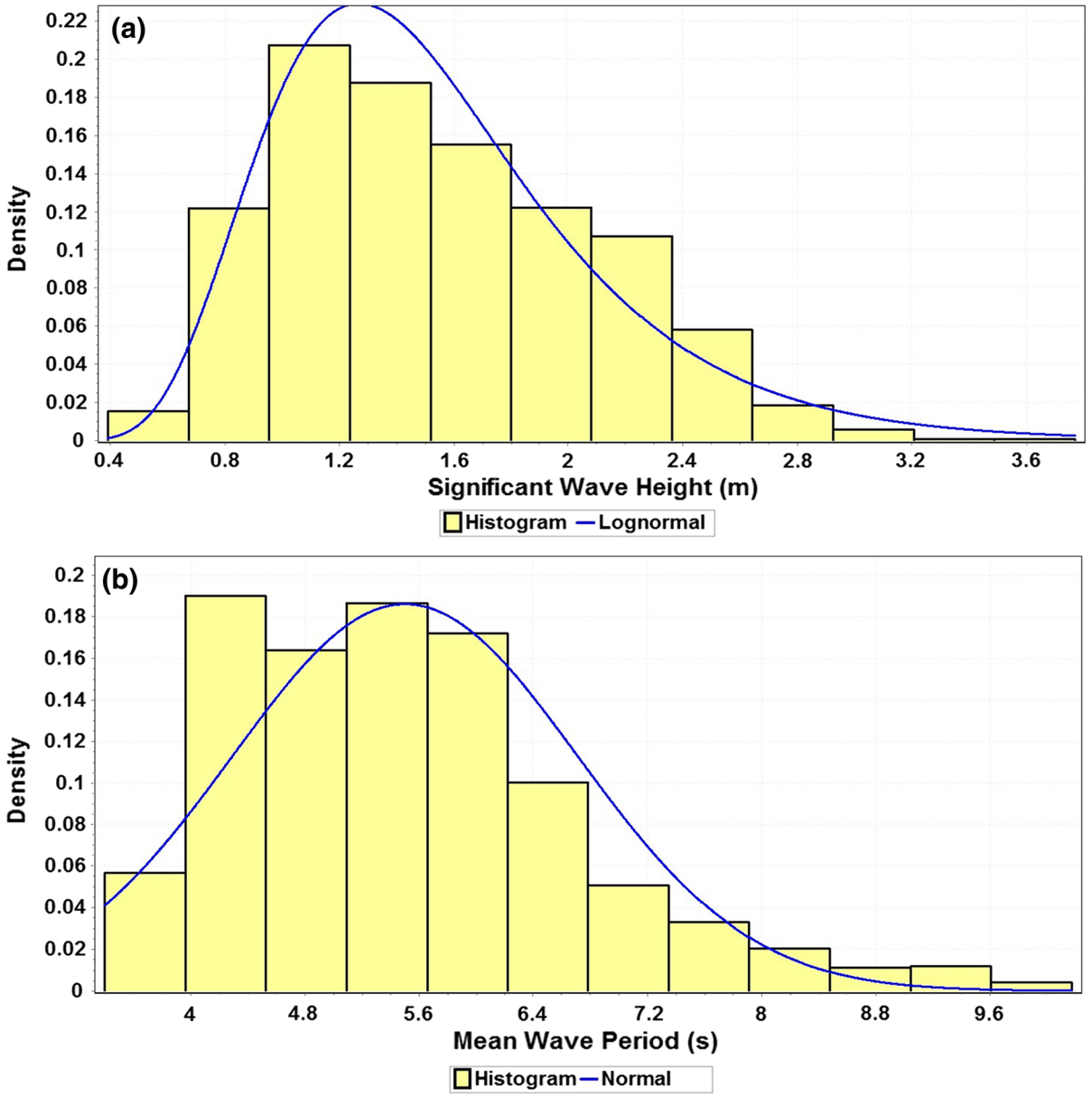

Figure 12
Probability density function (PDF) of **a** significant wave height and **b** mean wave period for Kulasekharapatnam

a better way to analyze the wave characteristics at the study area. The following are the conclusions from this study:

- From the modeling study, it is apparent that the wave parameters follow measurements reasonably well for different seasons. Statistical measures such as bias, R, RMSE, and SI are proven significant for the study period. Significant wave height ($R = 0.97$) and mean wave period ($R = 0.95$) follows the same pattern at the study location, with high agreement for wave directions throughout the year. For the post-monsoon and northeast monsoon periods, the comparison with buoy observations for significant wave height shows negative bias with moderate correlations. The

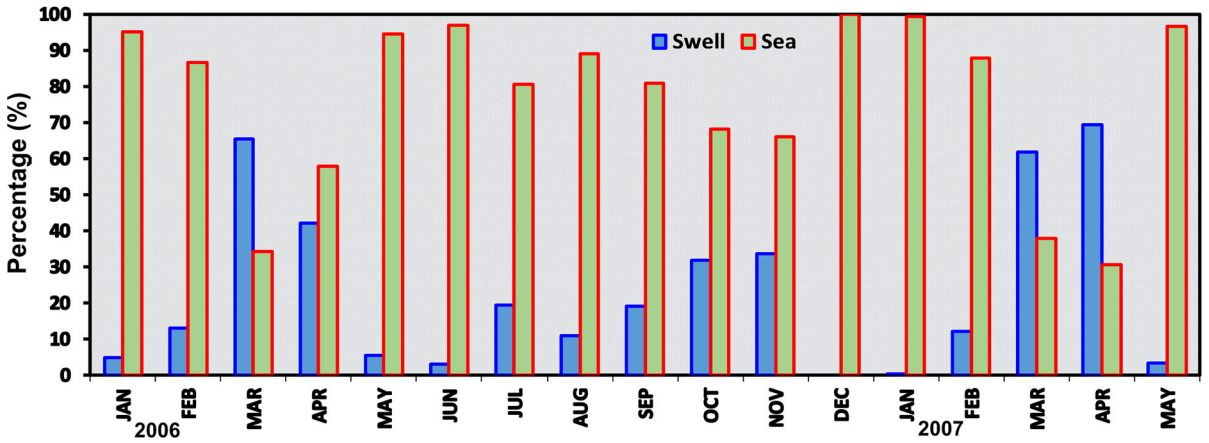

Figure 13
Percentage of swell and sea based on wave steepness for different months for the period from January 2006 to May 2007

southwest monsoon and post-monsoon seasons show correlation of 0.95 and 0.84, respectively. In addition, the RMSE varied from 0.13 to 0.38 m for the whole seasons that signifies a good fit. Correspondingly, for mean wave period, SI varied from 0.05 to 0.12, with a higher correlation for the southwest monsoon ($R = 0.97$). Overall, the model's performance during northeast monsoon was comparatively lower, due to the prevailing weak winds and generally not reproduced by any of the weather prediction models so far. In addition, it can be concluded that the significant wave height is less than 2.48 m for almost 95%; only 25% of time the wave heights are more than 1 m. To support this, it is evident that 25% of the waves were with wave period more than 4.54 s and 95% of the waves were with wave period more than 7.85 s.

- The sensitivity of the SWAN model to GEN3 physics and bottom friction parametrizations was tested by forcing the model with blended wind fields. The results of the study determined that the most accurate formulation for GEN3 physics in the SWAN model off Kulasekharapatnam is the Janssen formulation in simulating significant wave height with good accuracies, and Komen for simulating mean wave period. During the monsoon season, when fluctuations in the amplitudes of the waves are generally high, the Janssen option is found to perform better. The accurate formulation of the energy dissipation due to wind growth and whitecapping of the waves is a major reason for this. The JONSWAP formulation for bottom friction produced the most accurate model results for both height and period compared with Madsen and Collins formulation.
- The classification of waves using wave steepness indicated that swells are predominant in Gulf of Mannar during non-monsoon period, and amid rest of the year wind sea dominates. The dominance of swell is maximum (69.4%) during March and dominance of wind sea is maximum (100%) during December. Maximum wind seas and swell were observed during southwest monsoon (87.1%) and post-monsoon periods (32.8%). However, the interaction between the swells and wind seas must be better explored further to get a better understanding.

Thus, from the overall study it can be inferred that further long term measurements at the site can prompt to detailed modeling studies, which will be beneficial for navigational and coastal engineering projects.

Acknowledgements

The authors express their sincere thanks to INCOIS (Indian National Centre for Ocean Information Services, Hyderabad), Ministry of Earth Sciences,

Government of India for the wave data used in this study.

References

Aboobacker, V. M., Vethamony, P., Sudheesh, K., & Rupali, S. R. (2009). Spectral characteristics of the near-shore waves off Paradip, India during monsoon and extreme events. *Natural Hazards, 49,* 311–323.

Anonymous. (2011). *Indian tide tables 2011, Indian and selected foreign Ports*. New Delhi: Survey of India, Government of India.

Ardhuin, F., Bertotti, L., Bidlot, J. R., Cavaleri, L., Filipetto, V., Lefevre, J. M., et al. (2007). Comparison of wind and wave measurements and models in the western Mediterranean sea. *Ocean Engineering, 34,* 526–541.

Booij, N., Ris, R. C., & Holthuijsen, L. H. (1999). A third generation wave model for coastal regions: 1. Model description and validation. *Journal of Geophysical Research, 104*(C4), 7649–7666.

Caires, S., & Sterl, A. (2005). A new non parametric method to correct model data: application to significant wave height from the ERA-40 re-analysis. *Journal of Atmospheric and Oceanic Technology, 22*(4), 443–459.

Castelle, B., Bonneton, P., Senechal, N., Dupuis, H., Butel, R., & Michel, D. (2006). Dynamic of wave induced currents over an alongshore non-uniform multiple-barred sandy beach on the Aquitanian Coast, France. *Continental Shelf Research, 26,* 113–131.

Cavaleri, L., & Sclavo, M. (2006). The calibration of wind and wave model data in the Mediterranean Sea. *Coastal Engineering Journal, 53*(7), 613–627.

Chandramohan, P., Kumar, V. S., & Nayak, B. U. (1993). Coastal processes along shore front of Chilka Lake, east coast India. *Indian Journal of Marine Science, 22,* 268–272.

Cherian, A., Chandrasekar, N., Gujar, A. R., & Rajamanickam, V. (2012). Coastal erosion assessment along the southern Tamil Nadu coast, India. *International Journal of Earth Science Engineering, 5*(2), 352–357.

Collins, J. I. (1972). Predictions of shallow-water spectra. *Journal of Geophysical Research, 77,* 2693–2707.

Dee, D. P. (2011). The ERA-Interim reanalysis: Configuration and performance of the data assimilation system. *Quarterly Journal of the Royal Meteorological Society, 137,* 553–597.

Dingemans, M. W. (1997). *Water wave propagation over uneven bottoms, part 1, linear wave propagation. Advance series in ocean engineering* (Vol. 13, p. 471). River Edge: World Science.

Gowthaman, R., Kumar, V. S., Dwarakish, G. S., Soumya, S. M., Singh, J., & Kumar, K. A. (2013). Waves in Gulf of Mannar and Palk Bay around Dhanushkodi, Tamil Nadu, India. *Current Science, 104,* 1431–1435.

Gowthaman, R., Sanil Kumar, V., Dwarakish, G. S., Shanas, P. R., Jena, B. K., & Singh, J. (2015). Nearshore waves and longshore sediment transport along Rameswaram Island off the east coast of India. *International Journal of Naval Architecture and Ocean Enginering, 7,* 939–950.

Gunther, H., & Behrens, A. (2011). *The WAM model–validation document version 4.5.3*. Teltow: Helmholtz-Zentrum Geesthacht (HZG), Centre for Materials and Coastal Research.

Hasselmann, K., Barnett, T. P., Bouws, E., Carlson, H., Cartwright, D. E., Enke, K., et al. (1973). Measurements of wind–wave growth and swell decay during the Joint North Sea Wave Project (JONSWAP). *Deutsche Hydrographische Zeitschrift Supplement, A, 8*(12), 1–95.

Kalnay, E., Kanamitsu, R., Kistler, R., Collins, W., Deaven, D., Gandin, L., et al. (1996). The NCEP/NCAR 40-year reanalysis project. *Bulletin of the American Meteorological Society, 77,* 437–471.

Komen, G. J., Hasselmann, S., & Hasselmann, K. (1984). On the existence of a fully developed wind-sea spectrum. *Journal of Physical Oceanography, 14,* 1271–1285.

Kumar, V. S., Anand, N. M., Kumar, K. A., & Mandal, S. (2003). Multipeakedness and groupiness of shallow water waves along Indian coast. *Journal of Coastal Research, 19,* 1052–1065.

Kumar, V. S., Kumar, K. A., & Raju, N. S. N. (2004). Wave characteristics off Visakhapatnam coast during a cyclone. *Current Science, 86,* 1524–1529.

Kumar, V. S., Pathak, K. C., Padnekar, P., Raju, N. S. N., & Gowthaman, R. (2006). Coastal processes along the Indian coastline. *Current Science, 91,* 530–536.

Loveson, V. J. (1994). *Geological and geomorphological investigations related to sea level variation and heavy mineral accumulation along the Southern Tamilnadu Beaches, India*. Unpublished Ph.D. thesis, Madurai Kamaraj University, Madurai.

Madsen, O. S., Poon, Y. K., & Graber, H. C. (1988). *Spectral wave attenuation by bottom friction: Theory*. Proc. 21th Int. Conf. Coastal Engineering, ASCE, pp. 492–504.

Mazaheri, S., Kamranzad, B., & Hajivalie, F. (2013). Modification of 32 years ECMWF wind field using QuikSCAT data for wave hindcasting in Iranian Seas. *Journal of Coastal Research*, *1*(65), 344–349.

Milliff, R. F., Large, W. G., Morzel, J., Danabasoglu, G., & Chin, T. M. (1999). Ocean general circulation model sensitivity to forcing from scatterometer winds. *Journal of Geophysical Research, 12,* 11337–11358.

Moeini, M. H., Etemad-Shahidi, A., & Chegini, V. (2010). Wave modeling and extreme value analysis off the northern coast of the Persian Gulf. *Applied Ocean Research, 32,* 209–218.

Nayak, S., Bhaskaran, P. K., Venkatesan, R., & Dasgupta, S. (2013). Modulation of local wind waves at Kalpakkam from remote forcing effects of Southern Ocean swells. *Ocean Engineering, 64,* 23–35.

Nayak, B. U., Chandramohan, P., & Sakhardande, R. K. (1992). Seasonal distribution of wave heights off Yanam on the east coast of India. *Indian Journal of the Institution of Engineers, 72,* 187–193.

Neetu, S., Shetye, S., & Chandramohan, P. (2006). Impact of sea breeze on wind-seas off Goa, west coast of India. *Journal of Earth System Sciences, 1*(15), 2031–2038.

Pillar, P., Guedes, S. C., & Carretero, J. C. (2008). 44-year wave hindcast for the North East Atlantic European coast. *Coastal Engineering, 55,* 861–871.

Pond, S., & Pickard, G. J. (1991). *Introductory dynamical oceanography* (2nd ed., p. 329). Oxford: Pergamon Press.

Portilla, J., Ocampo-Torres, F. J., & Monbaliu, J. (2009). Spectral partitioning and identification of wind sea and swell. *Journal of Atmospheric and Oceanic Technolology, 26,* 117–122.

Prasad Kumar, B., Pang, I. C., Rao, A. D., Kim, T. H., Nam, J. C., & Hong, C. S. (2003). Seastate hindcast for the Korean seas with a spectral wave model and validation with buoy observation

during January 1997. *Journal of the Korean earth science society, 24,* 7–21.

Prasad Kumar, B., & Stone, G. W. (2007). Numerical simulation of typhoon wind forcing in the Korean seas using a spectral wave model. *Journal of Coastal Research, 23,* 362–373.

Premkumar, K., Ravichandran, M., Kalsi, S. R., Sengupta, D., & Gadgil, S. (2000). First results from a new observational system over the Indian seas. *Current Science, 78,* 323–330.

Rao, N. S. B., & Mazumdar, S. (1996). A technique for forecasting storm waves. *Indian Journal of Meteorology and Geophysics, 1996*(17), 333–346.

Reddy, M. P. M. (2001). *Descriptive physical oceanography* (p. 440). A.A. Balkema Publishers: Mangalore. ISBN 90-5410-706-5.

Ris, R. C. (1997). Spectral modelling of wind waves in coastal waters. (Ph.D. thesis, Delft University Press, Netherlands), p 160.

Saket, A., Etemad-Shahidi, A., & Moeini, M. H. (2013). Evaluation of ECMWF wind data for wave hindcasting in Chabahar zone. Proceedings of 12th International Coastal Symposium (Plymouth, England), *Journal of Coastal Research*, Special Issue 65, pp. 380–385.

Schneggenburger, C., Gunther, H., & Rosenthal, W. (2000). Spectral wave modeling with non-linear dissipation: Validation and applications in a coastal tidal environment. *Coastal Engineering, 41,* 201–235.

Senan, R., Anitha, D. S., & Sengupta, D. (2001). *Validation of SST and wind speed from TRMM using north Indian Ocean moored buoy observations*. CAOS Report 2001AS1, Centre for Atmospheric Sciences, Indian Institute of Science, Bangalore, India.

Sengupta, D., Goswami, B. N., & Senan, R. (2001). Coherent intraseasonal oscillations of ocean and atmosphere during Asian Summer monsoon. *Geophysical Research Letters, 28,* 4127–4130.

Signell, R. P., Carniel, S., Cavaleri, L., Chiggiato, J., Doyle, J. D., Pullen, J., et al. (2005). Assessment of wind quality for oceanographic modelling in semi-enclosed basins. *Journal of Marine Systems, 53,* 217–233.

Sorensen, R. M. (1997). *Basic coastal engineering*. New York: Springer Science.

Sundar, V., & Ananth, P. N. (1988). Wind climate for Madras harbor, India. *Journal of Wind Engineering and Industrial Aerodynamics, 31,* 323–333.

Swain, J. (1997). *Simulation of wave climate for Indian Seas*. Ph.D. thesis, Cochin University of Science and Technology, India.

Thompson, T. S., Nelson A. R., & Sedivy, D. G. (1984). *Wave group anatomy.* Proceedings of 19th Conference on Coastal Engineering, American Society of Civil Engineers, vol. 1, pp. 661–677.

Tolman, H. L. (1991). A third generation model for wind waves on slowly varying, unsteady and inhomogeneous depths and currents. *Journal of Physical Oceanography, 21,* 782–797.

Venkatesan, R., Lix, J. K., Phanindra, R. A., Arul, M. M., & Atmanand, M. A. (2016). Two decades of operating the Indian moored buoy network: significance and impact. *Journal of Operational Oceanography, 9*(1), 45–54.

WAMDIG. (1988). The WAM model—A third generation ocean wave prediction model. *Journal of Physical Oceanography, 18,* 1775–1810.

Wang, D. W., & Hwang, P. A. (2011). An operation method for separating wind sea and swell from the ocean wave spectra. *Journal of Atmospheric and Oceanic Technology, 18,* 2052–2062.

(Received December 9, 2016, revised June 19, 2017, accepted June 21, 2017, Published online June 29, 2017)